EFDA–JET–PR(12)07

A. Murari, M. Gelfusa, T. Lesage, D. Mazon, G.Arnoux
and JET EFDA contributors

# On the Potential of Information Theoretic Indicators for the Detection of Image Vibrations and for Image Registration on JET

# On the Potential of Information Theoretic Indicators for the Detection of Image Vibrations and for Image Registration on JET

A. Murari[1], M. Gelfusa[2], T. Lesage[3], D. Mazon[4], G. Arnoux[5]
and JET EFDA contributors*

***JET-EFDA, Culham Science Centre, OX14 3DB, Abingdon, UK***

*[1]Consorzio RFX-Associazione EURATOM ENEA per la Fusione, I-35127 Padova, Italy.*
*[2]Associazione EURATOM-ENEA - University of Rome "Tor Vergata", Roma, Italy.*
*[3]Arts et Metiers ParisTec Boulevard de l'Hopital 75013*
*[4]Association EURATOM-CEA, CEA Cadarache, 13108 Saint-Paul-lez-Durance, France*
*[5]EURATOM/CCFE Fusion Association, Culham Science Centre, Abingdon, Oxon OX14 3DB, UK*
** See annex of F. Romanelli et al, "Overview of JET Results",*
*(23rd IAEA Fusion Energy Conference, Daejon, Republic of Korea (2010)).*

Preprint of Paper to be submitted for publication in
IEEE Transactions on Plasma Science

**ABSTRACT**

In Tokamaks the use of cameras as diagnostics has increased remarkably in the last years. One of the main technical difficulties, in interpreting the data of camera based diagnostics, is the presence of movements and vibrations of the field of view, consequence of various plasma phenomena and modes of operation. Typically, these movements results in rigid transformations of the frames. In this paper various information theoretic indicators (correlations, entropies and mutual information) are described and their potential to detect the vibrations and to register images is investigated. The indicators are applied to a representative set of videos collected by JET wide angle infrared camera. For movement detection the Tsallis entropy is the indicator with the best performance, providing a success rates in excess of 86% and an almost equal number of false and missed detections. Its application to image registration looks also very promising.

## 1. THE PROBLEM OF VIBRATION DETECTION AND IMAGE REGISTRATION IN TOKAMAKS

In general "image registration" can be considered a form of data integration, in the field of image processing. Image registration indeed typically consists of transforming different sets of data into one coordinate system. The data to be integrated can come from many sources ranging from multiple photographs, from different sensors, from different times, or from different viewpoints. Applications are quite wide spread: computer vision, military, earth sciences are among the most relevant.

In Tokamaks, the main purpose of image registration is quite technical and consists of compensating for movements in the camera and/or their optics. Indeed during typical experiments, there are several potential sources of movements and vibrations in video frames. They can be due to the operation of the devices, for example rapid variations in the magnetic fields, or plasma phenomena, such as instabilities such ELMs and disruptions [1]. All these sources of perturbations typically cause only translations or rotations of the field of view and do not introduce distortions in the camera images. Some other specificities of the problem of image registration in Tokamaks must also be considered. First of all, the optical systems are too complex and the accessibility strongly limited, so that direct measurements of the vibrations is not a viable alternative [2]. Moreover, the changes in the background illumination are so strong that no reference points are reliably available inside the field of view. These properties of the movements restrict strongly the class of methods that can be usefully applied.

Image movement detection and image registration can be classified into intensity-based and feature-based techniques. Typically one of the images is referred to as the *reference* and the second image is referred to as the *target*; image registration is performed by spatially transforming the target image to align with the reference image. Intensity-based methods use suitable correlation metrics. Feature-based methods find correspondence between image reliable features such as points, lines, and contours. Knowing the correspondence between a number of points in images, a transformation is then determined to map the target image to the reference images, thereby establishing point-

by-point correspondence between the reference and target images. As mentioned, in Tokamak, the background illumination changes too much even during the same discharge for feature-based methods to be viable.

Image registration techniques comprise two main categories also in terms of the transformation performed to register. The first broad category of transformation models includes linear transformations such as translation, rotation and scaling. These are global in nature, which means that they operate in the same way on all pixels. The second category of transformations include 'no rigid' transformations, which are designed to locally warp the target image to align with the reference image. No rigid transformations include radial basis functions (thin-plate or surface splines, multiquadrics, and compactly-supported transformations), physical continuum models (viscous fluids), and large deformation models. In Tokamaks, the frames of the cameras are typically affected by rigid movements and therefore only the first class of techniques will be considered in the following

Irrespective of the nature of the problem affecting the image stability, both movement detection and image registration are based on image similarity. The accuracy of both detection and registration depend therefore on the criterion used to determine the similarity. An image similarity measure quantifies the degree of similarity between intensity patterns in two images. In this paper various information theoretic criteria are used as similarity measures. They belong to two main categories: cross correlations and mutual information (see section 2 for the details).

An alternative and complementary approach consists performing the difference between the two images to register and analyse the statistical distributions of the residuals, the differences pixel per pixel. In this perspective various types of entropies have been investigated (again see section 2 for the details).

These two classes of indicators have been tested first with rectangular matrices of natural numbers, to double-check the proper implementation of the codes and to get familiar with their behaviour. Then they have been applied to a database of videos collected on JET by the wide angle infrared camera, which provides an overview of the inner wall. The potential of the various indicators to detect movements of the frames has been assessed in detail. The first attempts at registration have also been performed but more statistics is required to identify with certainty the most suitable indicator for this application.

With regard to the structure of the paper, in the next section the mathematical expressions of the used 8 indicators are described in detail. To familiarise ourselves with the behaviour of these indicators in the case of images (2D signals), their application to numerical cases is the subject of section 3. After describing JET wide angle camera and the used database in section 4, section 5 and 6 are devoted to the description of the results obtained in detecting vibrations using the experimental videos. In section 7 the best indicator, the Tsallis entropy, is applied to the problem of image registration, using both synthetic and actual frames. The directions of future investigations are the subject of the last section 8 of the paper.

## 2. THE MATHEMATICAL FORMULATION OF THE USED INDICATORS

### *2.1 CROSS-CORRELATION*

In signal processing, the cross-correlation is a measure of similarity of two waveforms as a function of a time-lag applied to one of them. The concept can be extended to 2 dimensions. The cross-correlation, and especially the normalized cross-correlation, is indeed a very effective indicator to determine the level of similarity between different images. Therefore the cross-correlation can be used to detect vibrations and register images.

The normalized cross-correlation is used in the rest of this paper to obtain results between 0 and 1. This makes it easier the post processing and the comparison with other methods. In the present application, the two images to analyze are indicated as f and g and their pixels have x, y coordinates. The functions $f(x,y)$ and $q(x,y)$ describe the intensity of the images. The basis of the cross-correlation method is the estimate of a distance measure, typically the squared Euclidean distance given by:

$$d^2_{f,t}(x,y) = \sum_{x,y} [f(x,y) - g(x,y)]^2 \tag{1}$$

The normalized cross-correlation NCC can be expressed as:

$$NCC = \frac{\sum_{x,y} [f(x,y) - \bar{f}) * (f(x,y) - \bar{g})]}{\sqrt{\left\{\sum_{x,y} [f(x,y) - \bar{f}]^2 * \sum_{x,y} (f(x,y) - \bar{g})]^2\right\}}} \tag{2}$$

Where $\bar{f}$ and $\bar{g}$ is the means of the function $f$ and $g$.

### *2.2 SHANNON ENTROPY*

Entropy is a basic thermodynamic concept which means that isolated systems in nature tend to degrade from order to disorder. In information theory, entropy is a measure of the uncertainly associated with a random variable. The concept was introduced by Claude E. Shannon in his 1948 paper "A Mathematical Theory of Communication" [3]. In this context, the term usually refers to the Shannon entropy, which quantifies the expected value of the information contained in a message - a 'message' means a specific realization of a random variable. Equivalently, the Shannon entropy is a measure of the average information content one is missing when one does not know the value of the random variable.

The Shannon entropy can be expressed as:

$$S(p) = -\sum_{i=1}^{n} p(x_i) * \log(p(x_i)) \tag{3}$$

Where

- $X$ is a random variable with k outcome $X = \{x_1, x_2, ..., x_n\}$.
- $p(x_i)$ is the probability mass function of $x_i$.

This definition of entropy can be easily applied also to images, if $p(x_i)$ is assumd to be the probability of the pixels having the value $x_i$.

### *2.3 TSALLY ENTROPY*

In information theory, other definitions of entropy have been developed after Shannon's. The most famous is probably the Tsallis entropy, with his generalization of the standard Blotzmann-Gibbs entropy, but there are other definitions which are detailed in this section.

In 1988, Constantino Tsallis introduced the $S_q$ entropy in his paper "*Possible generalization of Boltzmann-Gibbs statistics*." The $S_q$ entropy generalizes the Shannon entropy to non-additive systems and adds a free parameter q, which characterizes the degree of non-additivity. This entropy definition was introduced into the physics literature, where it has become quite important in statistical mechanics and atomic physics because of its ability to describe non-extensive processes that are common at many physical levels. The Tsallis entropy can be expressed as:

$$S_q(p) = \frac{1}{q-1} * (1 - \sum_{i=1}^{n} p(x_i)^q) \tag{4}$$

Where

- q is a real parameter which is a measure of non-extensitivity.
- $X$ is a random variable with k outcome $X = \{x_1, x_2, ..., x_n\}$.
- $p(x_i)$ is the probability mass function of $x_i$.

For the applications described in this paper, the best value of the parameter q has proved to be 0.1. One of the main reasons for the introduction of $S_q$ is the modelling of system with long term correlations. $S_q$ is well suited to this goal, because different values of the free parameters q alter the relative importance of the various probabilities. For example, a q much less than 1 tends to emphasize the role of the smaller probabilities. In our application, the free parameter q will be chosen to maximize the chances of properly detecting the movements of the camera field of view and compensate them. Indeed, selecting a small value for the parameter q, the $S_q$ entropy becomes much more sensitive than traditional Shannon entropy to long range correlations. This sensitivity to long term correlations, obtained for appropriate values of the free parameter q, is essential for vibration detection and image registration in JET. Indeed when an object moves in the field of view of a camera, in the difference between two subsequent frames mainly short range correlation appear. On the other hand, if the entire frame has moved, in the difference between two frames long range structures tend to appear and they can be detected by the Tsallis entropy [2].

### *2.4 RENYI ENTROPY*

The Renyi entropy [5] of order q, $S_q$was one of the first generalized entropies to gain widespread attention. It is expressed as:

$$R_q(X) = \frac{1}{q-1} * \log\left(\sum_{i=1}^{n} p_i^{\,q}\right) * q \in R\backslash\{0,1\} \tag{5}$$

Again different values of the free parameters q alter the relative importance of the various probabilities.

### *2.5 ALPHA ENTROPY*

The difference between two probability distributions can be expressed by a so-called measure of divergence [6]. A specific class of divergence measures, the f-divergence, is particularly useful in our context and can be expressed as:

$$f(P\|Q) = \sum_i q_i f\left(\frac{p_i}{q_i}\right) \tag{6}$$

Where $$q_i f\left(\frac{p_i}{q_i}\right) = \begin{cases} 0_i & if\ p_i = 0, p_i = 0 \\ p_i\, lim_{x\to\infty} \frac{f(x)_i}{x} & if\ p_i > 0, p_i = 0 \end{cases}$$

A special case of f-divergence includes the $I_\alpha$−divergence measures. These are defined similarly to f-divergence measures, but apply only to specific probability distributions. They are a measure of the distance between a given joint probability $p_{ij}$ and the joint probability when the variables are independent ($p_i p_j$). The definition of the alpha entropy used in this paper is:

$$I_\alpha(X\|Y) = \frac{1}{\alpha(\alpha-1)} * \sum_{x,y}\left(\frac{p^\alpha(x,y)}{(p(x)*(p(y)^{\alpha-1}} - 1\right) \quad if\ \alpha \in R\backslash\{0,1\} \tag{7}$$

### *2.6 MUTUAL INFORMATION*

In probability theory and information theory, the mutual information of two random variables is an indicator that quantifies the mutual dependence of the two random variables. In our case, the mutual information quantifies the resemblance of two images.

The mutual information of two images X and Y can be defined as:

$$MI(X,Y) = \sum_x \sum_y p(x,y) * \log\left(\frac{p(x,y)}{(p(x)*(p(y)}\right) \tag{8}$$

where $p(x, y)$ is the joint probability distribution function of X and Y, and $p(x)$ and $p(y)$ are the marginal probability distribution functions of X and Y respectively.

The mutual information of relation (8), can also be expressed in terms of the Shannon definition of entropy:

$$MI(X, Y) = S(X) + S(Y) - S(X,Y) \tag{9}$$

where $S(X)$ and $S(Y)$ are the Shannon entropies, and $S(X, Y)$ is the joint Shannon entropy of $X$ and $Y$. The mutual information can also be expressed, using the Tsallis, entropy as:

$$MI_T(X, Y) = S_T(X) + S_T(Y) + (1-q) * S_T(X) * S_T(Y) - S_T(X, Y) \tag{10}$$

Where $Sq(X)$ and $Sq(Y)$ are the Tsallis entropies, and $Sq(X,Y)$ is the joint Tsallis entropy of $X$ and $Y$

Thus, the normalized mutual information based on nonadditive Tsallis entropy $I_N$ is expressed as:

$$MI_{NT}(X,Y) = \frac{MI_T}{\max(S_T(X), (S_T)(Y)) + (1-q) * (S_T(X) * S_T(Y)_)} \tag{11}$$

The mutual information can also be extended using the Renyi entropy $I_N$ as:

$$I_{NR}(X,Y) = \frac{R_q(X) + R_q(Y)}{R_q(X,Y)} \tag{12}$$

where $R_q(X)$ and $R_q(Y)$ are the Renyi entropies, and$R_q(X, Y)$ is the joint Renyi entropy of $X$ and $Y$.

## 3. APPLICATION TO A GENERIC MATRIX

The aim of this section is to understand the behaviour of the indicators introduced in the previous section, using a simple numerical synthetic case. This first step has been performed by applying the various indicators on synthetic examples –namely a 50×50 matrix. The squared matrices of numbers simulate the images. This first step has helped to identify the proper range for the values of free parameters of the indicators such q and $\alpha$.

In more detail, to calculate the indicators, the procedure consists of several steps:

– The first one is to generate one matrix 50×50 as show below:

$$\begin{pmatrix} 1 & 2 & 3 & \dots & 49 & 50 \\ 2 & 3 & 4 & \dots & 50 & 1 \\ \vdots & \vdots & \vdots & \vdots & \vdots & \vdots \\ \vdots & \vdots & \vdots & \vdots & \vdots & \vdots \\ 49 & 50 & 1 & \dots & \dots & 48 \\ 50 & 1 & 2 & \dots & \dots & 49 \end{pmatrix} = \text{A0}$$

– Then, at each iteration (up to 50), the matrix is shifted of one row at the time and it is substitute with one row of random numbers. For example the first step could generate the following matrix:

$$\begin{pmatrix} 12 & 28 & 45 & \dots & 21 & 32 \\ 1 & 2 & 3 & \dots & 50 & 1 \\ \vdots & \vdots & \vdots & \vdots & \vdots & \vdots \\ \vdots & \vdots & \vdots & \vdots & \vdots & \vdots \\ 48 & 49 & 50 & \dots & \dots & 47 \\ 49 & 50 & 1 & \dots & \dots & 48 \end{pmatrix} = \text{A1}$$

– As the last step the various indicators are calculated considering the first matrix as the reference for all iterations. The entropies are calculated for the difference between the matrix at a certain iteration and the reference matrix. Correlation and mutual information are also calculated comparing the matrix at a certain iteration and the reference matrix

The result for the NCC is shown in figure 1. As expected, the maximum value is at the beginning of the test. Indeed, at the first iteration, the two consecutives matrices are just different in the first row. At the last iteration, the two matrices are almost completely different.

In figures 2, the Shannon entropy and the mutual information (using the Shannon definition of entropy) are plotted. They show the expected trends but the sensitivity is not very high.

In the case of Tsallis definition of entropy, to evaluate the influence of the free parameter, several curves are plotted in figure 3 for different values of q, namely $\{0.1, 0.5, 0.9, 1.5, 3\}$. We can see that the best results are obtained for the value $q = 0.1$, since this shows the highest difference between the values of the entropy at the beginning and the end of the curve. In figure 3 the mutual nformation using Tsallis definition of entropy is compared to the one obtained using Shannon entropy, proving gain the higher sensitivity of the entropy with parameter $q = 0.1$.

In figure 4 the same exercise has been performed for the Renyi definition of entropy and the relative mutual information. Various values of q have been explored, namely $\{0.1, 0.5, 2, 3\}$. The best value turns out to be $q = 0.5$, again because this shows the highest difference between the values at the beginning and at the end of the curve.

The same type of test has also been carried out for the alpha entropy. The results are shown in figure 5. In this case, we find that the best value for alpha is the highest.

## 4. JET DIAGNOSTIC AND THE ANALYSED DATABASE

The information theoretic indicators, introduced in the previous sections, have been applied to the videos collected by JET wide angle InfraRed (IR) camera. The camera measures the infrared emission from JET first wall in the wavelength range 3.5-5μm. To avoid damage, the camera is located at the end of the endoscope shown in figure 6. The first optical component of the endoscope is a parabolic mirror then a Cassegrain telescope is located just before the camera. A Cassegrain telescope is a combination of a primary concave mirror and a secondary convex mirror.

The wide angle IR camera was installed on JET in September 2005 and its measurements are of great interest because they show in a very immediate way how Plasma Facing Components (PFC) heat up during a pulse. The wide angle infrared camera is a digital camera, shoes sensor is a 560×600 pixel array. The software allows the user to set Regions Of Interest (ROIs). Smaller ROIs allow the camera to capture at faster speeds. The camera has two separate output channels: the live video and the digital channel: only the video channel is available in real time and it is the one used for the investigations presented in this paper.

During a discharge, various plasma events and operational conditions can cause the endoscope and/or the camera to move. For precision sake, it is worth mentioning that in the paper the generic term camera movement is used. This is in the interest of simplicity and readability of the paper, because in reality the movements of the field of view of the wide angle IR camera can be due also to oscillations or bending of the entire endoscope. This distinction is immaterial to the objective of the present paper, which is simply aimed at describing methods to automatically identify movements of the field of view and register the affected frames, independently from the physical origins of these movements. In any case, given the high number of optical components and the reduced accessibility, the solution of measuring directing the movements affecting the videos is not feasible. A typical image recorded by the camera is shown in figure 7.

To obtain the statistical results exported in the following sections, videos from a database contains of 69 videos and 35939 frames has been built and analysed. All these frames have been analysed manually and in 7948 of them ( corresponding to 22%) some sort of rigid movement has been detected visually. These movements are typically translations in the vertical and/or horizontal direction.

## 5. COMPARISON OF THE DIFFERENT INDICATORS WHEN APPLIED TO JET VIDEOS

The various indicators introduced in section 2 have been deployed to analyse actual videos of JET wide angle camera. The main purpose of this investigation is to understand the behaviour of the various indicators and their performance when applied to actual videos of JET wide angle camera. . With regard to the comparison of the various entropies, the Tsallis and Renyi definitions have been particularised for $q = 0.1$, because this value proves to be the best value for the application discussed in this paper (see also section 6).

The time evolution of the various entropies for a typical JET video is reported in figure 8. The vertical lines indicate the part of the discharge in which the video is affected by vibrations. All the entropies of the difference between a frame and the previous one show a clear change in value in the region of the vibrations.

For the same discharges, the time evolution of the NCC and the various definition of the Mutual Information have also been compared as shown in figure 9; again the vertical lines indicate the region with vibrations and movements of the frames.

It is worth mentioning that a systematic investigation of the results with various values of the free parameter $\alpha$ has been undertaken also for the quantity $I_\alpha$. Unfortunately, in the case of JET videos, it has not been possible to find a value of this quantity providing sensible and interesting results. For this reason, this quantity cannot be applied to JET videos and will not be discussed further in this paper.

## 6. STATISTICAL RESULTS FOR THE DETECTION OF MOVEMENTS

The evolutions of the various indicators with time suggest a way to use them for movement detection.

For each quantity an appropriate threshold is identified, which allows an efficient discrimination between frames with and without vibrations. An example of the idea is illustrated in figure 10, in which a threshold is optimised for a discharge and for the Tsallis entropy $S_q$.

The approach of course has to be optimised for the entire database and not only for a single video. To this end, a realistic range of values for the thresholds, as determined by a manual analysis of the main videos, has been scanned to identify, for each information theoretic quantity, the best threshold to separate frames with vibrations from those without. The final best results obtained, for each indicator, have been compared. They are reported in table I.

Table I Comparison of the success rates for the optimised thresholds of the various indicators. The last column indicates the ranking of the various indicators in terms of global success rate, false positives and false negatives.

## 7. THE USE OF THE INDICATORS FOR REGISTRATION

The aim of the registration is to re-adjust frames which have shifted. Indeed the long term objective of this investigation is to detect and correct the vibrations affecting videos of JET cameras. A quite extensive survey of the movements of the IR wide angle camera has shown that the frames are mainly affected by vertical and horizontal displacements. On the other hand, rotations have practically never been detected. Therefore the tested algorithm for the moment implements corrections only for translations in these two directions. The registration consists of displacing the frame to be registered in the horizontal direction until a minimum of the entropy or a maximum in the mutual information is found. Then the operation is repeated for the vertical direction. The cycle is repeated a couple of times. For the small displacement affecting the videos of the wide angle IR camera, this procedure has proved to be more than adequate. In the next subsection this approach is tested first on a purely numerical matrix and then on some typical videos.

### *7.1 REGISTRATION OF A MATRIX*

To verify the effectiveness of the approach and compare the various indicators in terms of registration efficiency, a first series of tests has been performed using synthetic frames. These frames are matrices of numbers: their rows and/or columns shifted of a known quantity. The indicators introduced in the previous sections are then deployed to detect the entity of this shift.

To fix the ideas, let's start with the following matrix: We have, firstly, the frame at time T:

$$Matrix\ (t = T) = M\ (T) = \begin{pmatrix} 1 & 2 & 3 & \dots & 49 & 50 \\ 2 & 3 & 4 & \dots & 50 & 1 \\ \vdots & \vdots & \vdots & \vdots & \vdots & \vdots \\ \vdots & \vdots & \vdots & \vdots & \vdots & \vdots \\ 49 & 50 & 1 & \dots & \dots & 48 \\ 50 & 1 & 2 & \dots & \dots & 49 \end{pmatrix}$$

Suppose the matrix at time T+1 is the matrix to be registered:

$$Matrix\,(t = T+1) = M\,(T+1) = \begin{pmatrix} / & / & / & \dots & / & / \\ / & 1 & 2 & \dots & 49 & 50 \\ \vdots & \vdots & \vdots & \vdots & \vdots & \vdots \\ \vdots & \vdots & \vdots & \vdots & \vdots & \vdots \\ / & 48 & 49 & \dots & \dots & 47 \\ / & 49 & 50 & \dots & \dots & 48 \end{pmatrix}$$

In the case of the entropies, to register this matrix ($M\,(T+1)$)it has to be shifted in the horizontal and vertical directions until a minimum in the entropy of the difference with respect to M(T) is found. A comparison of the results for the three definitions of entropy used so far is reported in figure 11.

The results obtained with the mutual information and the normalized cross-correlation are shown on the figure 12.

In general, for these numerical cases, the Tsallis definition of entropy and the Mutual Information based on Tsallis entropy tend to provide the best results. Indeed, as can be seen in the figures, they are more sensitive than the other indicators to small displacements of a few rows and/or a few columns. In figure 13, the results of these two operators are compared, showing that the Mutual Information based on Tsallis entropy is the most promising of the two.

### *7.1 REGISTRATION OF JET IMAGES*

The procedure described in the previous section has also been applied to some JET videos. Since from the analysis reported in section 6, the Tsallis entropy and mutual information seem to be the most sensitive indicators, these are the indicators which have been considered for the first attempts of registration.

One example investigated is the shot 73851. The evolution of the Tsallis definition of entropy is reported in figure 14. Vibrations have been detected manually between approximately frame 600 and frame 900.

The procedure of alternatively shifting an image in the horizontal and vertical direction has been applied to Frame 787. This frame has been registered with respect to the previous one 786. In figure 7, the evolutions of the mutual information with Tsallis entropy depending on direction (left, right, up and down) are plotted.

In figure 15, it can be seen that mutual information has a maximum for a shift of 2 pixels in the right direction. In all the other directions, the indicator decreases with the shift. Therefore it is reasonable to assume that the second frame is shifted that the shift between the two frames is two rows rightwards.

Figure 16 shows the difference of the two frames before and after the correction. The white pixels indicate the difference between the two frames. After the corrections, the remaining features due to the main structures of the wall are clearly reduced. This proves that the correction ha a positive effect and that the mutual information with the Tsallis entropy identify the right registration which has to be implemented.

A similar set of tests has also been performed for the case of the Mutual information with the Tsallis definition of entropy. Very similar results have been obtained for both indicators.

## 8. FUTURE PERSPECTIVES

The analysis of various information theoretic indicators has provided quite interesting results. The Tsallis entropy clearly outperforms all the other entropies and similarity measures at the task of identifying movements in the field of view of JET wide angle IR camera. The same indicator is also very powerful in identifying the shift in the horizontal and vertical direction to be used to register the frames affected by movements. The normalised correlation and the mutual information, using the Tsallis definition of the entropy, give also reasonable results but prove inferior in this application. With regard to the registration, the Tsallis entropy and the mutual information with the Tsallis entropy provide interesting and very comparable results. Further investigations are required to identify the best indicator for JET application.

With regard to future applications, it is planned to apply the same indicators to different cameras on JET, which show larger movements. Some cameras indeed show also rotations. In some case the movements of the frames are much larger than the few pixels, as is the case for the wide angle IR camera. These more severe problems are expected to require significant refinements of the techniques described in this paper.

## ACKNOWLEDGMENTS

This work, supported by the European Communities under the contract of Association between EURATOM/ENEA and CEA, was carried out under the framework of the European Fusion Development Agreement. The views and opinions expressed herein do not necessarily reflect those of the European Commission.

## REFERENCES

[1]. J. Wesson "Tokamaks" Oxfrod University Press, 4th Edition 2011

[2]. A. Murari, D. Mazon, A. Debrie "*On the use of Non-additive Entropy to determine the presence of vibrations in the videos of JET cameras*" IEEE Transactions on plasma science Volume: PP Issue:99, page(s): 1 - 7 ISSN: 0093-3813, Septembre 2011.

[3]. C.E. Shannon, Warren Weaver. *The Mathematical Theory of Communication*. Univ of Illinois Press, 1949. ISBN 0-252-72548-4

[4]. C. Tsallis "*Possible generalization of Boltzmann–Gibbs statistics*" Journal of Statistical Physics, vol. **52**, pp. 479–487.

[5]. A.Renyi "*On measures of information and entropy*". Proceedings of the 4th Berkeley Symposium on Mathematics, Statistics and Probability 1960. pp. 547–561. http://digitalassets.lib.berkeley.edu/math/ucb/text/math_s4_v1_article-27.pdf.

[6]. JosienP.W.Pluim, J.B.A, and M. A. Viergever, f-information Measures in Medical Image registration, IEEE Transactions on Medical Imaging, Vol **23**, Issue 12, 2004, 1508-1516

| | Threshold | Correct detection | Missed movements | False movements |
|---|---|---|---|---|
| Normalized cross-correlation | 0.94 | 81.38 | 14.84 | 3.78 |
| Shannon entropy | 1.6 | 84.17 | 15.35 | 0.48 |
| Shannon mutual information | 0.62 | 78.09 | 0.47 | 21.44 |
| Tsallis entropy | 25 | 86.19 | 6.66 | 7.15 |
| Tsallis mutual information | 0.58 | 79. 98 | 0.48 | 19.54 |
| Renyi entropy | 8 | 84.70 | 15.14 | 0.16 |
| Renyi mutual information | 1.28 | 79.80 | 2.58 | 17.62 |

*Table I shows that the Tsallis entropy is the best indicator. It achieves the best results in terms of total success rate. Moreover it provides also the best balance between false and mixed detections.*

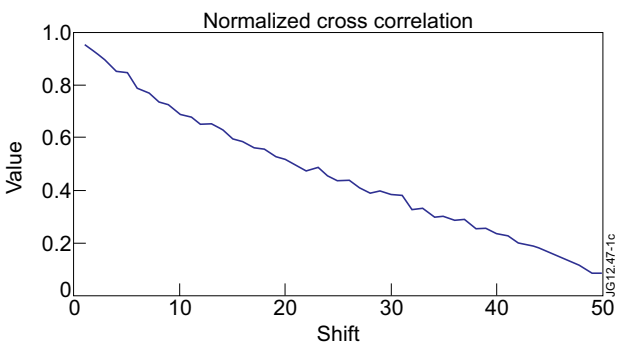


*Figure 1. Trend of the NCC at various shifts of the image.*

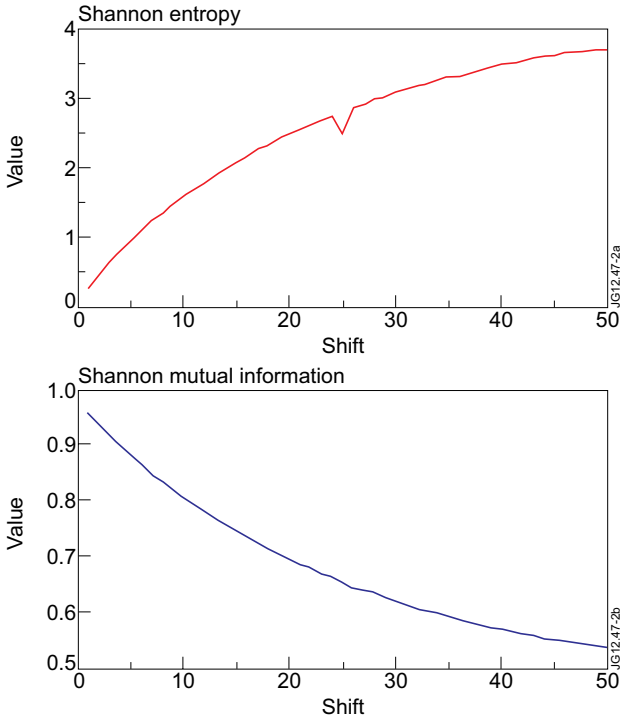


*Figure 2. Trend of the Shannon entropy and the mutual information using the Shannon definition of entropy at various shifts of the image.*

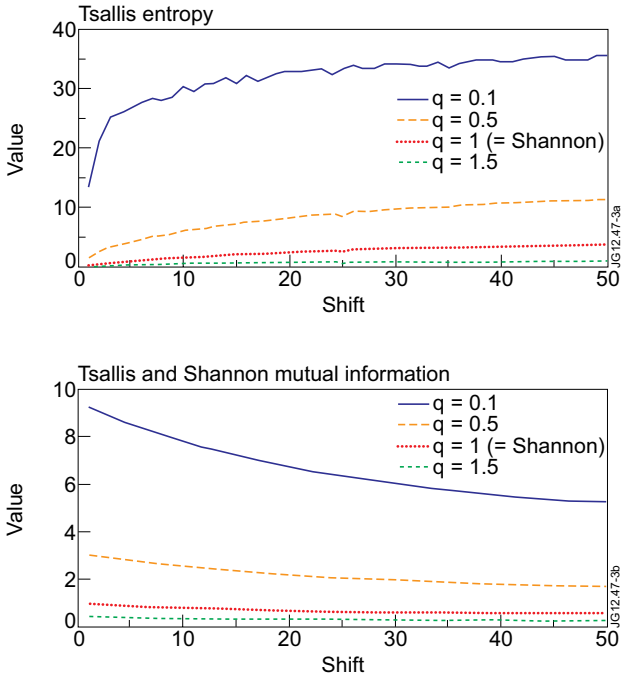


*Figure 3. Trend of the Tsallis entropy (top) and the mutual information (bottom) using the Tsallis definition of entropy at various shifts of the image.*

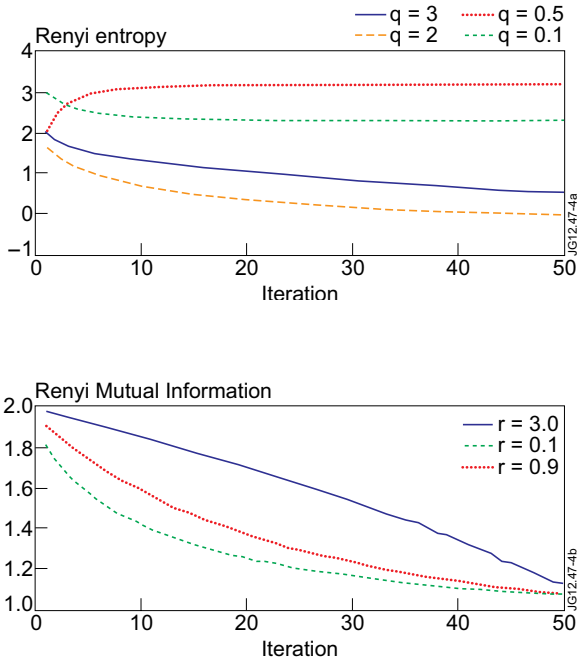


*Figure 4: Trend of the Renyi entropy (top) and the mutual information (bottom) using the Renyi definition of entropy at various shifts of the image.*

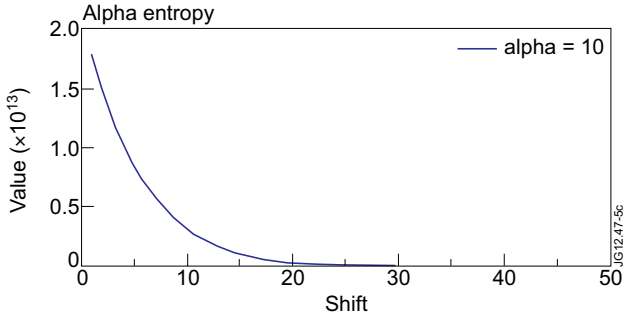


*Figure 5: Alpha entropy for α=10.*

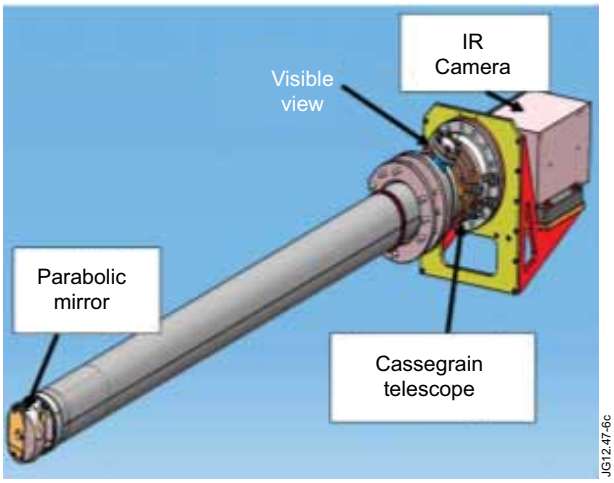


*Figure 6: Camera configuration.*

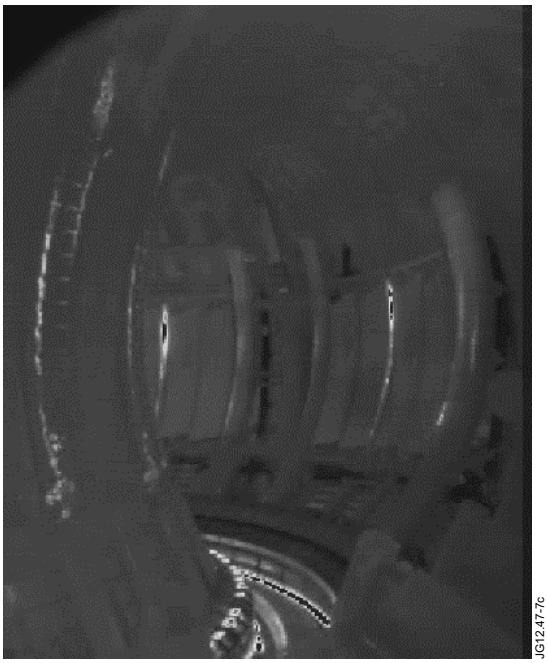


*Figure 7: Typical image of the first wall as taken by the IR wide angle camera.*

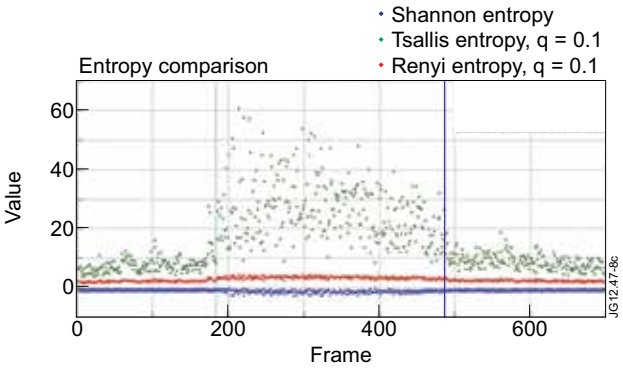


*Figure 8: Comparison of different entropies for Pulse No: 68815. The x axis is the frame number and therefore can be assimilated to time.*

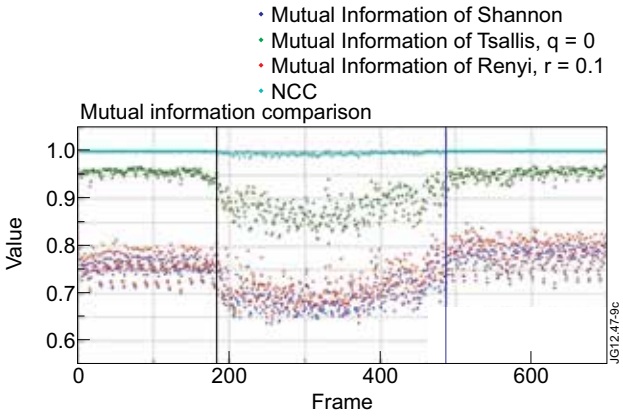


*Figure 9: Comparison of the normalised cross correlation and the different definitions of the Mutual information for Pulse No: 68815. The x axis is the frame number and therefore can be assimilated to time.*

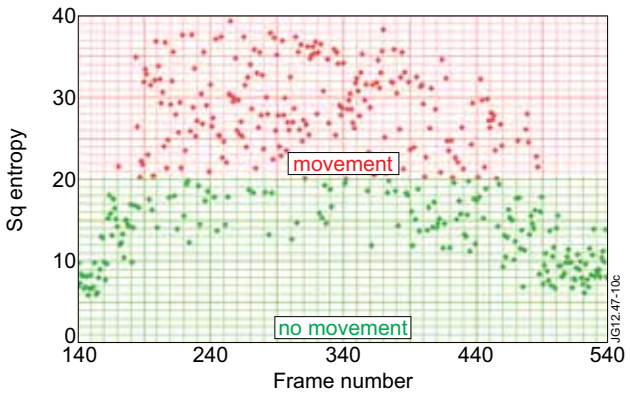


*Figure 10: Example of the definition of a threshold for a single video.*

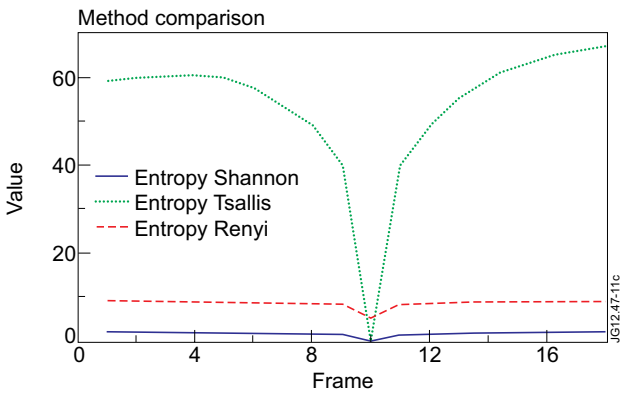


*Figure 11: Comparison between different definition of entropy.*

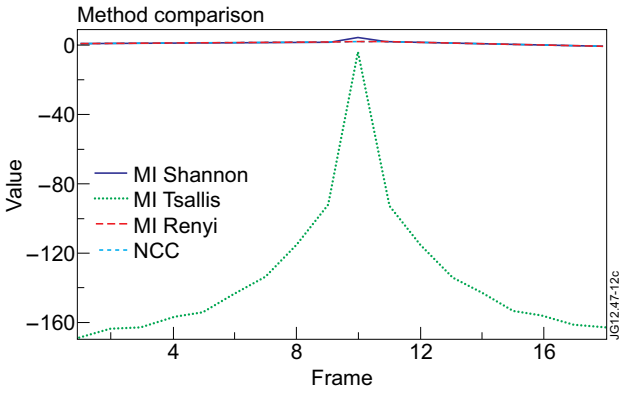


*Figure 12: Comparison between different definition of mutual information and normalized cross-correlation.*

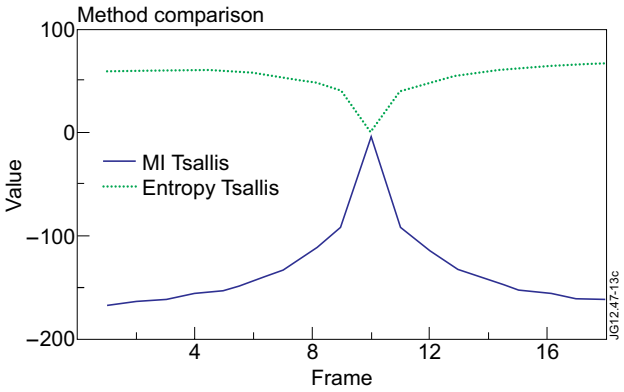


*Figure 13: Comparison between mutual information and Tsallis entropy.*

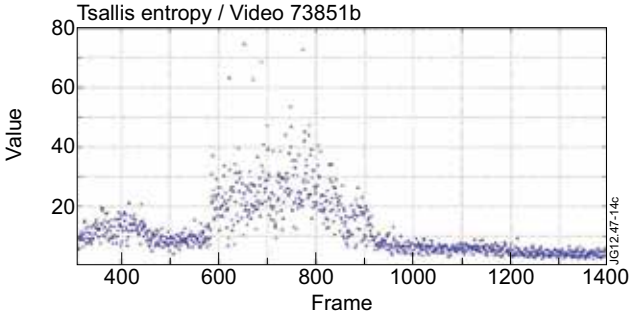


*Figure 14: Evolution of the Tsallis entropy for Pulse No: 73851. Vibrations occur between approximately frame 600 and frame 900*

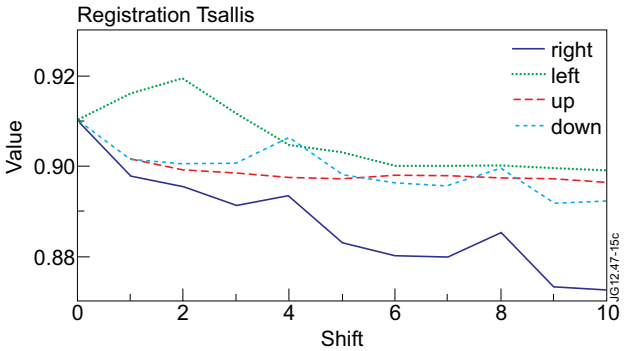


*Figure 15: Registration of video of video 787, Pulse No: 73851.*

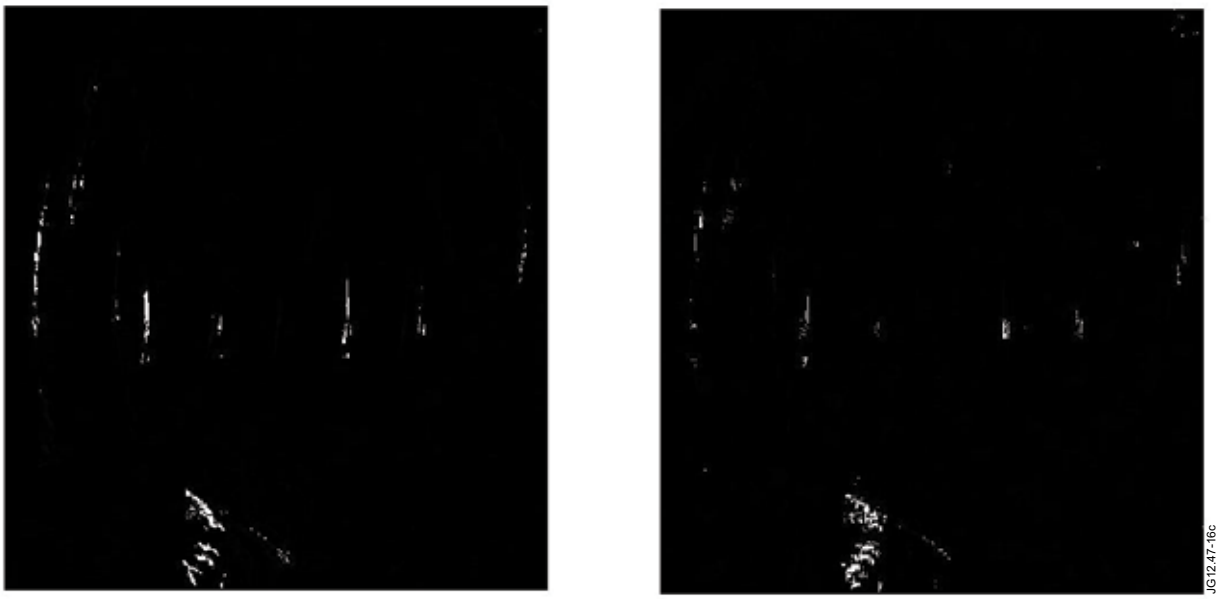


*Figure 16: Difference between frame 787 and frame 786.*